

On the performance of iterative receivers for interfering MIMO-OFDM systems in measured channels

P. Hammarberg*, P. Salvo Rossi†, F. Tufvesson*, O. Edfors*, V.-M. Kolmonen‡,
P. Almers*, R.R. Müller†, A. F. Molisch*

*Department of Electrical and Information Technology, Lund University, Lund, Sweden.

†Dept. of Electronics and Telecommunications, Norwegian University of Science and Technology, Trondheim, Norway.

‡Radio Laboratory, Helsinki University of Technology, Helsinki, Finland.

Abstract—This paper investigates the gains harvested through base station cooperation in the up-link for a multi-user (MU) Multiple-Input Multiple-Output Orthogonal Frequency Division Multiplexing (MIMO-OFDM) system, operating in a real indoor environment. The base stations perform joint detection using an iterative receiver that carries out multi-user detection and channel estimation via soft information from the single-user decoders. Performance evaluation is carried out using real channels from an indoor dynamic dual MIMO link measurement campaign. The measured scenario represent a real life situation where two users communicate with two base stations, each with two antennas, in an environment resembling a shopping mall or an airport terminal. System performance is evaluated in terms of both Bit-Error Rate (BER) vs. Signal-to-Interference Ratio (SIR) and Cumulative Distribution Functions (CDF) for the instantaneous BER. Also, the impact of using soft information in the channel estimation is analyzed.

I. INTRODUCTION

Multiple-Input Multiple-Output (MIMO) systems in combination with Orthogonal Frequency Division Multiplexing (OFDM) and iterative receivers have gained interest in current wireless communication research. MIMO-OFDM [1] systems can simultaneously mitigate inter-symbol interference and enhance system capacity through increased diversity, spatial multiplexing or interference suppression. At the same time iterative receivers, implementing Multi-User Detection (MUD) and channel estimation, achieve near-optimum performance with reasonable complexity [2].

In this paper we evaluate an iterative receiver for MIMO-OFDM systems using real channel measurements from an indoor dynamic dual-link scenario assuming a “quasi-static”, i.e. block-fading, channel. The receiver performance has earlier been evaluated in [3], where focus was on analyzing Bit-Error Rate (BER) performance at different Signal-to-Interference Ratios (SIR). This paper focus on how the receiver can be used for interference mitigations through base station cooperation. By combining the received signals from two base stations a virtual antenna array is created that allow for joint detection of the two users. In this paper a system with two users and

This work has been supported by the Research Council of Norway (NFR), the Swedish Governmental Agency for Innovation Systems (VINNOVA), and the Finnish Funding Agency for Technology and Innovation (TEKES), under the project WILATI within the NORDITE framework.

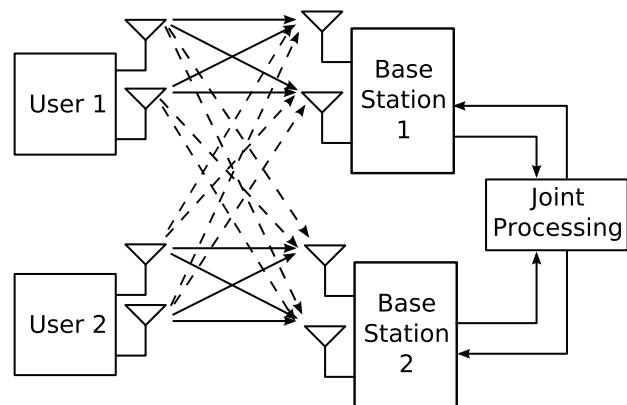


Fig. 1. The considered multi-user system with cooperative detection.

two base stations, each with two antennas, is considered. The system is shown in Fig. 1. Evaluation of the BER performance at different SIR levels is performed both with and without cooperating base stations. Additionally, an analysis of the impact of using soft information, obtained by decoding the received symbols, in the channel estimator is performed.

II. SYSTEM MODEL

A MIMO-OFDM system with K transmit and N receive antennas is considered, where each transmit antenna sends an independent data stream. The transmit/receive antennas may belong to different users/base stations. Each stream is encoded via convolutional coding and random interleaving, with code-words spanning both time and frequency dimensions. OFDM symbols with pilot data are inserted for channel estimation at the receiver. QPSK modulation is considered, and each frame (codeword + pilots) consists of L bits grouped in S OFDM symbols of M subcarriers each. The frame structure is shown in Fig. 2.

Referring to the m th subcarrier during transmission of the s th OFDM symbol, we denote the transmitted vector, the channel matrix, the AWGN vector, and the received vector as

$$\mathbf{x}[m, s] = (x_1[m, s], \dots, x_K[m, s])^T,$$

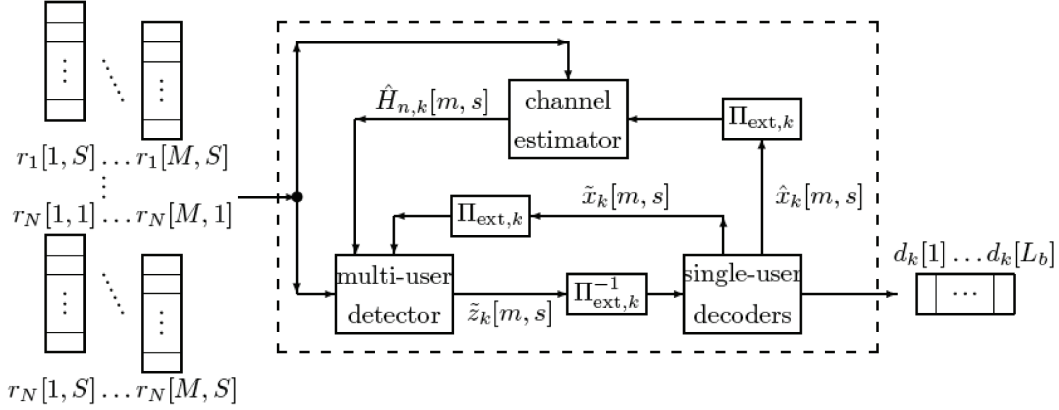


Fig. 3. The structure of the iterative receiver.

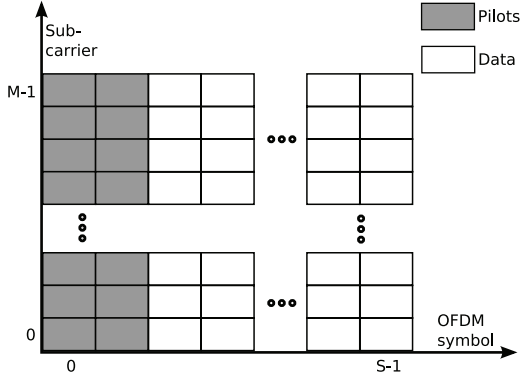


Fig. 2. M subcarrier OFDM frame structure with, in this case, two pilot symbols followed by $S-2$ data symbols.

$$\mathbf{H}[m, s] = \begin{pmatrix} H_{1,1}[m, s] & \dots & H_{1,K}[m, s] \\ \vdots & \ddots & \vdots \\ H_{N,1}[m, s] & \dots & H_{N,K}[m, s] \end{pmatrix},$$

$$\mathbf{w}[m, s] = (w_1[m, s], \dots, w_N[m, s])^T, \text{ and}$$

$$\mathbf{r}[m, s] = (r_1[m, s], \dots, r_N[m, s])^T.$$

The discrete-time model for the received signal can then be written as

$$\mathbf{r}[m, s] = \mathbf{H}[m, s]\mathbf{x}[m, s] + \mathbf{w}[m, s]. \quad (1)$$

Note that \mathbf{H} contains the coefficients for both useful and interfering channels and that synchronous transmissions are assumed. The channel vector from the k th transmit antenna is denoted $\mathbf{h}_k^{(\text{tx})}[m, s]$.

At the receiver, as illustrated in Fig. 3, OFDM symbols are demodulated and sent to the iterative decoder, performing MUD, Soft-Input Soft-Output (SISO) decoding and channel estimation. The multiuser detector and SISO decoders exchange extrinsic information on symbols x_k , denoted \tilde{x}_k (resp. \tilde{z}_k) when going to the multiuser detector (resp. the SISO decoders). SISO decoders also provide *a posteriori* information

on symbol x_k , denoted \hat{x}_k , to the channel estimator, and *a posteriori* information on source bits. The channel estimator provides channel coefficient estimates ($\hat{H}_{n,k}$).

A. MUD

The received signals (1) are processed separately for each subcarrier and OFDM symbol. Parallel interference cancellation is performed using \tilde{x} from the SISO decoders and $\hat{\mathbf{H}}$ from the channel estimators. The residual term from the interference cancellation for the k th transmit antennas, $\tilde{\mathbf{r}}^{(k)} = \mathbf{r} - \hat{\mathbf{H}}(\tilde{\mathbf{x}} - \hat{x}_k \mathbf{i}_K^{(k)})$, is then MMSE filtered, to reduce noise and multi-user interference, giving the extrinsic information

$$\tilde{z}_k = \frac{\mathbf{i}_K^{(k)T} \left(\hat{\mathbf{H}}^H \hat{\mathbf{H}} + \sigma_w^2 \mathbf{V}^{(k)} \right)^{-1} \hat{\mathbf{H}}^H \tilde{\mathbf{r}}^{(k)}}{\mathbf{i}_K^{(k)T} \left(\hat{\mathbf{H}}^H \hat{\mathbf{H}} + \sigma_w^2 \mathbf{V}^{(k)} \right)^{-1} \hat{\mathbf{H}}^H \mathbf{h}_k^{(\text{tx})}}, \quad (2)$$

with $\mathbf{V}^{(k)} = \text{diag}((1 - |\tilde{x}_1|^2), \dots, 1 - |\tilde{x}_{k-1}|^2, 1, 1 - |\tilde{x}_{k+1}|^2, \dots, 1 - |\tilde{x}_K|^2)$. For the derivation we refer to [2].

B. SISO Decoding

After collecting $\{z_k[\ell]\}_{\ell=1}^L$, each transmit antenna can be decoded independently using the log-domain BCJR algorithm. The SISO decoder for the k th transmit antenna uses the model $z_k = x_k + v_k$, with $v_k \sim \mathcal{N}_{\mathbb{C}}(0, \eta_k^2)$ and $\eta_k^2 = \frac{1}{\mathbf{i}_K^{(k)T} (\mathbf{H}^H \mathbf{H} + \sigma_w^2 \mathbf{I}_N)^{-1} \mathbf{H}^H \mathbf{h}_k^{(\text{tx})}}$.

C. Channel Estimation

Assuming that the maximum normalized delay spread ($\eta_{\text{max}}^{(d)}$) is known, the receiver implements a low-complexity estimator based on the Slepian expansion

$$H_{n,k}[m] \approx \sum_{i=1}^I \psi_{n,k}[i] v_i[m],$$

where $\psi_{n,k}[i]$ is the i th Slepian coefficient for the link between the k th transmit antenna and the n th receive antenna; $v_i[m]$ is the m th sample of the i th time-shifted Discrete

Prolate Spheroidal (DPS) sequence associated to the interval $m = 1, \dots, M$ with time support $[0, \eta_{\max}^{(d)}]$ with corresponding eigenvalue $\lambda_i^{(d)}$; the approximate signal space extension is $\lceil \eta_{\max}^{(d)} M \rceil + 1 \leq I \leq M$. See [4] for more details. Also, we denote $\mathbf{v}[m] = (v_1[m], \dots, v_I[m])^T$, $\boldsymbol{\lambda}^{(d)} = (\lambda_1^{(d)}, \dots, \lambda_I^{(d)})^T$, $\Xi[m, s] = \mathbf{I}_N \otimes (\mathbf{x}[m, s] \otimes \mathbf{v}[m])^T$, $\boldsymbol{\psi}_{n,k} = (\psi_{n,k}[1], \dots, \psi_{n,k}[I])^T$, where \otimes denotes the Kronecker product. The signal model for channel estimation is

$$\mathbf{r} = \Xi \boldsymbol{\psi} + \mathbf{w},$$

with \mathbf{r} , Ξ , $\boldsymbol{\psi}$ and \mathbf{w} appropriately collecting received signals, transmitted signals, Slepian coefficients and noise.

A linear MMSE estimate is performed

$$\hat{\boldsymbol{\psi}} = \left(\hat{\Xi}^H \boldsymbol{\Delta}^{-1} \hat{\Xi} + \mathbf{C}_{\boldsymbol{\psi}}^{-1} \right)^{-1} \hat{\Xi}^H \boldsymbol{\Delta}^{-1} \mathbf{r},$$

where $\mathbf{C}_{\boldsymbol{\psi}}$ is the diagonal correlation matrix of the Slepian coefficients depending on the eigenvalues; $\hat{\Xi}$ contains the expected transmitted symbols computed via *a posteriori* information from SISO decoders; $\boldsymbol{\Delta}$ is a diagonal matrix depending on the *a posteriori* information from the SISO decoders and the SNR.

III. DYNAMIC MULTI-LINK MIMO CHANNEL MEASUREMENTS

A. Dynamic Multi-link MIMO Channel Measurements

The channel measurements [5] used in this evaluation were carried out in September 2007 in the CS-building at *Helsinki University of Technology*, Finland. The building is a modern four story building with corridors and offices surrounding a large atrium in the middle, resembling an airport terminal or a shopping mall. A mobile transmitter and two stationary receivers were used to measure the behavior of the dynamic multi-link channel. Fig. 4 shows a photograph of the building with both the receiver locations and the two transmitter routes marked.

The measurement setup is summarized here, and the basic measurement parameters are found in Table I. In order to capture the behavior of the multi-link MIMO scenario, a single signal was transmitted from the transmitter to both receiving channel sounders. The transmitter was moved along several routes with a speed of about 1 m/s, and the MIMO channel transfer function was sampled each 39 ms. Sixteen dual-polarized antennas were used at each link end and local rubidium clocks in the channel sounders were used for synchronization.

TABLE I
MEASUREMENT PARAMETERS.

Center frequency	5.3 GHz
Bandwidth	120 MHz
TX power	0.5 W (27 dBm)
Gap between MIMO blocks	39.3216 ms

In order to create a scenario with multiple users and base stations, measurements from two different routes of the mobile

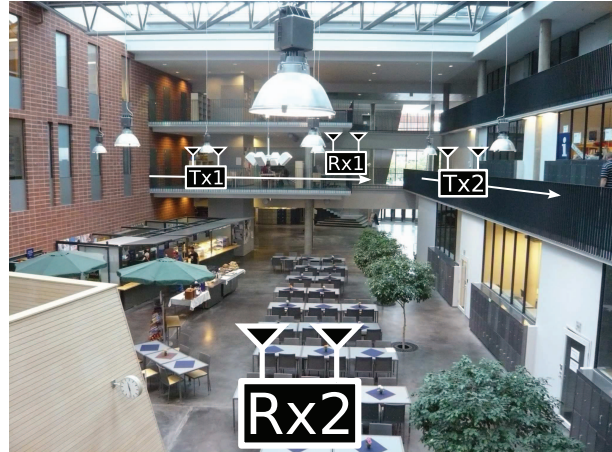


Fig. 4. Photograph of the measurement location. The receivers (Rx1 and Rx2) are static, while the transmitters (Tx1 and Tx2) move along the paths indicated by arrows.

transmitter were combined. Even though these measurements were performed at different time instances, the environment is considered static between the measurements; thus the measurements are treated as co-located in time. The resulting channel data files from the measurements include two 32×32 MIMO channels per receiver. From these, four 2×2 MIMO channels were extracted, two for each receive and transmit combination. The combined channel represent the links between two mobile users and two base stations, with two antennas each.

The upper part of Fig. 5 displays a map of the considered scenario, showing the location of the static transmitters and moving receivers. The light gray area is the atrium area and the white area indicate the second floor where the measurements took place.

B. Processing of Channel Measurements

Post processing of the data has been performed in order to reduce the measurement noise present in the channel data. Further, interpolation has been performed in order to change the original frequency spacing in the measurements (0.6250 MHz) to a subcarrier spacing of 0.3125 MHz, in accordance with the recent IEEE 802.11n WLAN proposal [6]. The processing was performed using an interpolating Wiener filter [7] in the frequency domain, assuming a rectangular power delay profile. In essence, the filter removes all energy beyond a certain delay. The maximum delay was chosen in such way that a reasonable noise reduction was obtained, while still preserving the channel energy.

A simple power control scheme was used in the simulation. The principles of the schemes were as follows; the average powers in the links between the users and their intended base station were normalized to unity for each channel realization. That is, the receive power from the primary user was held constant at the base stations. At the same time the interfering links were scaled by the same amount, preserving the relative power levels of the measured channel. Fig. 5 shows the average

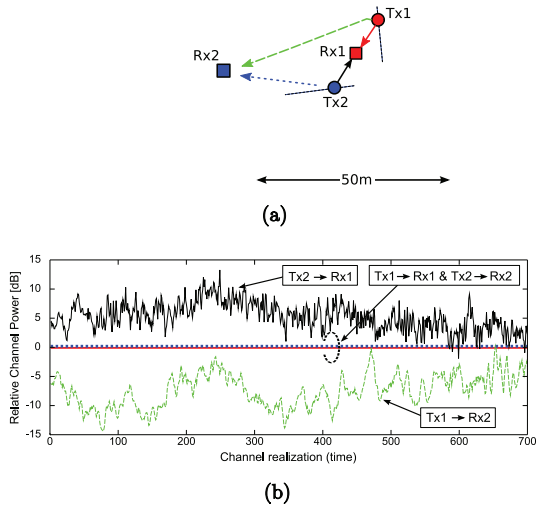


Fig. 5. Part (a) displays a map of the measurement location showing the position of the receivers (Rx) and the routes of the transmitters (Tx). The arrows represent the signal paths from the transmitters to the receivers. In part (b) the average power in the different links, for the different channel realizations, after power control.

power in each link, as indicated on the map, after the power control scheme has been applied.

IV. RESULTS

As mentioned above, the system under consideration consists of two mobile users and two base stations, each with two antennas. The two users send independent codewords from each antenna spanning $S = 10$ OFDM symbols, including $S_p = 2$ OFDM pilot symbols, where each OFDM symbol contains $M = 64$ subcarriers (see Fig. 2). The channel is considered to be static over several frames, and each frame covers one code word. Code bits are generated by a rate 1/2 recursive systematic convolutional encoder [8] with generators $(7, 5)_8$ and with two tail bits forcing the final state into 1, giving 1020 information bits per frame and user. Assuming an OFDM symbol duration of $4\mu s$ [6], each user in the considered system transmits at a rate of $25.6 Mbps$.

System simulations have been conducted in order to investigate the gains harvested through base station cooperation. Both the case of no cooperation, meaning that the inter-user interference is ignored at the receiver, and the case of full cooperation are treated. Results are presented in terms of the BER as a function of SIR, as well as in terms of the Cumulative Distribution Function (CDF) of the instantaneous BER at each channel realization. In the simulations a fixed receiver noise variance is set to give an E_b/N_0 of $5dB$ per receiver branch.

It is worth noting that for the case of base station cooperation, it is in this case somewhat misleading to talk about SIR, since the interference actually becomes useful signals power that can be used for detecting the transmitted signals. This additional power will also cause the effective E_b/N_0 to vary depending on the received power in the interfering link.

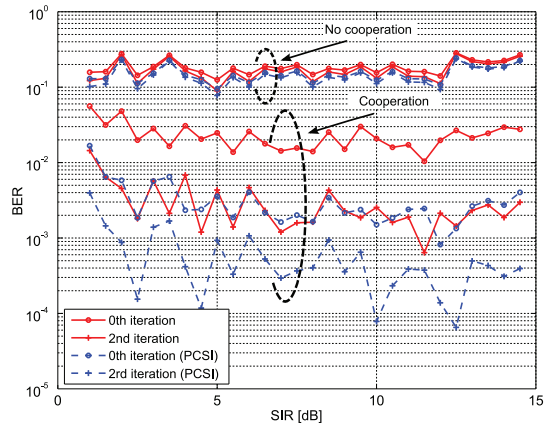


Fig. 6. BER versus SIR with and without base station cooperation. The results shows the performance after the $0th$ and $2nd$ iteration. The case of PCSI is shown with dashed lines.

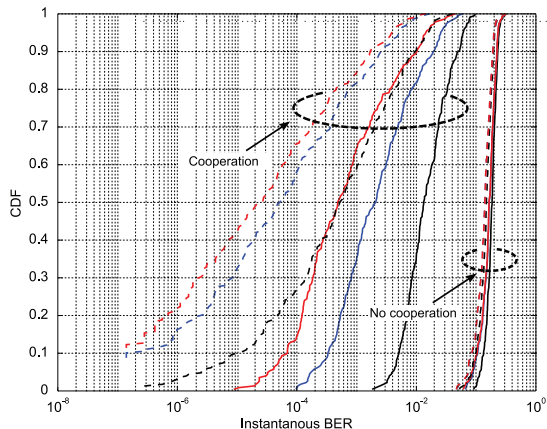


Fig. 7. CDF of instantaneous BERs, with and without base station cooperation. The performance after the $0th$, $1st$ and $2nd$ iteration is shown. The case of PCSI is shown with dashed lines.

In Fig. 6 the performance for the user with the most favorable interference situation (Rx2 in Fig. 5) is shown for both with and without base station cooperation, after the $0th$ (when performing spatial filtering only) and $2nd$ iteration. As a comparison, the performance with Perfect Channel State Information (PCSI) at the receiver is shown. A sliding window mean taken over the different instantaneous SIR values has been performed to obtain the presented results.

Additional insight of the behavior of the system can be found by looking at the CDF of the instantaneous BER. Fig. 7 shows the CDF calculated from 230 individual channel realizations, corresponding to different positions of the users. The figure shows the performance after the $0th$, $1st$ and $2nd$ iteration, both with and without cooperation. Again the case of PCSI is shown for comparison.

Considering the performance with no cooperation, the interference and noise levels are so severe that the performance of

the system is very poor. From Fig. 6 it is seen that the BER only reach values in the order of 10^{-1} . Looking at Fig. 7, it is seen that the variance of the BER values is small; thus the performance is relatively independent of the individual channel realizations in the evaluated scenario. It is also seen that with PCSI the performance is still poor, though slightly better than when estimating the channel. Further, the gain obtained by performing iterations in the receiver is small. One iteration gives a small gain, but performing yet another iteration has an insignificant impact.

If instead the two base stations are allowed to cooperate, joint detection of the two users greatly improve performance. As can be seen in Fig. 6 the performance after two iterations are almost two orders of magnitude better than for the case of no cooperation. From Fig. 7 it can be seen that there is a significant performance difference between different channel realizations. Depending on the structure of the channel, and the total available power in the link, the instantaneous BER performance is seen to differ more than one order of magnitude between different measured channel realizations. This difference is growing considerably with iterations, while the average BER decreases.

It can also be seen that the difference in BER performance between PCSI and an estimated channel decreases with iterations. This is explained by the reduction of the channel estimation error due to improvements of the soft information with iterations.

In order to show the impact of using soft information in the channel estimation, performance simulations have been performed using only the known pilots in the estimator. Fig. 8 shows the CDF of the BER when using, and not using, soft information. The results are for the case of base station cooperation, after the 0th, 1st and 2nd iteration. The performance is, as expected, identical before starting iterations, differing only due to independent noise realizations. When using only known pilots, the gain of performing more than one iteration is insignificant. If instead soft information is used to update the channel estimate, performance improve with every iteration. When designing MIMO-OFDM systems, this property can be used to decrease the amount of pilots transmitted, thereby decrease pilot overhead and increase spectral efficiency.

V. CONCLUSION

A performance evaluation of an iterative receiver for MU-MIMO-OFDM has been performed, focusing on how the algorithm can be used for base station cooperation in the up-link. Computer simulations have been performed using real channels from an indoor dynamic dual-link MIMO measurement campaign. The considered system has two users and two base stations, all with two antennas.

It has been seen that by allowing the two base stations to cooperate in the detection of the two users, large gains are achieved. When there is no cooperation, the interference and noise severely limits performance and iterations in the receiver do not give any significant performance gains. On the other hand, if base stations are allowed to cooperate a significant performance increase is achieved. Especially if iterations are

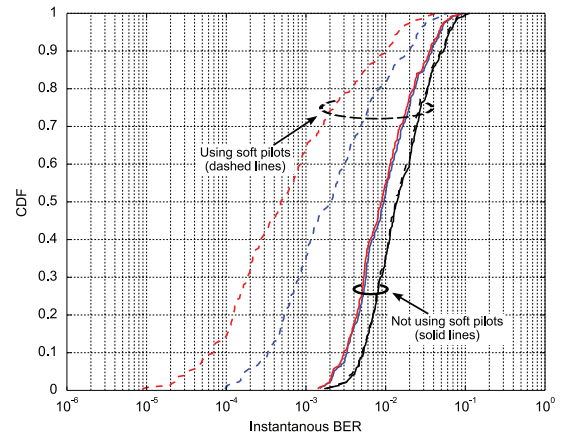


Fig. 8. CDF of the BER when using (dashed lines), and not using (solid lines), soft information in the channel estimator. The results are for the case of base station cooperation, and shows performance after the 0th, 1st and 2nd iteration. As expected, the performance is identical for the two cases after the 0th iterations.

performed, making use of soft information for channel estimation and interference cancellation. The performance gain in terms of BER is orders of magnitude. Using soft information in the estimator also open up the possibility of reducing the overhead in terms of transmitted pilot symbols, yielding increased spectral efficiency.

REFERENCES

- [1] G.L. Stüber, J.R. Barry, S.W. McLaughlin, Y. Li, M.A. Ingram, T.G. Pratt, "Broadband MIMO-OFDM Wireless Communications," *Proc. IEEE*, vol. 92(2), pp. 271–294, Feb. 2004.
- [2] T. Zemen, C.F. Mecklenbräuker, J. Wehinger, R.R. Müller, "Iterative Joint Time-Variant Channel Estimation and Multi-User Detection for MC-CDMA," *IEEE Trans. Wireless Commun.*, vol. 5(6), pp. 1469–1478, Jun. 2006.
- [3] P. Salvo Rossi, P. Hammarberg, F. Tufvesson, O. Edfors, P. Almers, V.M. Kolmonen, J. Koivunen, K. Haneda, R.R. Müller, "Performance of an Iterative Multi-User Receiver for MIMO-OFDM Systems in a Real Indoor Scenario," *IEEE GLOBECOM*, to appear in Dec. 2008.
- [4] D. Slepian, "Prolate Spheroidal Wave Functions, Fourier Analysis, and Uncertainty - V: The Discrete Case," *Bell System Technical Journal*, vol. 57, no. 5, pp. 1371–1430, May/June 1978.
- [5] J. Koivunen, P. Almers, V.-M. Kolmonen, J. Salmi, A. Richter, F. Tufvesson, P. Suvikunnas, A.F. Molisch, P. Vainikainen, "Dynamic multi-link indoor MIMO measurements at 5.3 GHz," *IEEE EuCAP*, Nov. 2007.
- [6] S. Coffey, A. Kasher, A. Stephens, "Joint Proposal: High Throughput Extension to the 802.11 Standard: PHY," *IEEE 802.11-05/1102r2*, January 2006.
- [7] S.M. Kay, *Fundamentals of Statistical Signal Processing: Estimation Theory*, Prentice Hall, 1993.
- [8] J.G. Proakis, *Digital Communications*, McGraw Hill, 2000.